communications earth & environment

Article

A Nature Portfolio journal

https://doi.org/10.1038/s43247-025-02541-5

Traces of the oxygen isotope composition of ancient air in fossilized cosmic dust

Fabian Zahnow [1,2] ✉, Martin D. Suttle [3,4], Marina Lazarov [5], Stefan Weyer[5], Tommaso Di Rocco [1], Luigi Folco [4] & Andreas Pack[1]

As a sub-type of micrometeorites, I-type cosmic spherules form by complete melting and oxidation of extraterrestrial Fe, Ni metal particles during their atmospheric entry. All oxygen in the resulting Fe, Ni oxides sources from the Earth's atmosphere and hence makes them probes for the composition of atmospheric oxygen. When recovered from sedimentary rocks, they allow the reconstruction of the triple oxygen isotope composition of past atmospheric O_2, providing quantitative constraints on past CO_2 levels or global primary production. Here we establish using fossil I-type cosmic spherules as an archive of Earth's atmospheric composition with the potential for a unique record of paleo-atmospheric conditions dating back billions of years. We present combined triple oxygen and iron isotope compositions of a collection of fossil I-type cosmic spherules recovered from Phanerozoic sediments. We reconstruct the triple oxygen isotope anomalies of past atmospheric O_2 and quantify moderate ancient CO_2 levels during the Miocene (~8.5 million years) and late Cretaceous (~87 million years). We also demonstrate this method's competitive precision for paleo-CO_2 determination, despite challenges in finding micrometer-sized unaltered fossil I-type cosmic spherules. Our work indicates that morphologically intact spherules can be isotopically altered by terrestrial processes, underscoring the need for rigorous sample screening.

Earth receives a continuous flux of small extraterrestrial particles. When hitting the Earth's atmosphere with hypervelocity, such particles are visible as shooting stars. The remnants of such objects are termed micrometeorites and comprise particles smaller than 2 mm[1]. Those micrometeorites that suffered complete melting in the upper atmosphere at 85 – 90 km are termed cosmic spherules[2]. Micrometeorites with terrestrial ages <2 Ma (hereafter referred to as modern) can be collected in Antarctica or even from roof tops, with the latter being called urban micrometeorites with very young decades or centuries long terrestrial ages. Geologically old fossil micrometeorites are preserved in sediments with the oldest record dating 2.7 Ga back in Earth's history[3–8]. Iron-rich I-type cosmic spherules are virtually the exclusive component in fossil micrometeorite collections due to their resistance to weathering[6]. The I-type cosmic spherules are composed of Fe, Ni oxides, namely wüstite (FeO) and magnetite (Fe_3O_4) and residual metal[9]. Their I-type micrometeorite precursor consists of Fe, Ni metal alloy, which is gradually oxidized in molten state during atmospheric interaction[9]. Thus, the entire oxygen in I-type cosmic spherules originates from the atmosphere, which is, e.g., CO_2 for the Archean or O_2 for younger samples after the Great Oxidation Event[10,11].

It has been demonstrated on Quaternary Antarctic I-type cosmic spherules that the triple oxygen isotope anomaly of air O_2 can be reconstructed from combined triple oxygen and iron isotope compositions[10,11]. Both, oxygen and iron in unaltered modern I-type spherules are enriched in heavy isotopes due to evaporation during atmospheric entry[10–12]. The iron isotopes are used in this approach as proxy for the degree of atmospheric evaporation, because iron is only affected by evaporation and, unlike oxygen, not by exchange with the atmosphere.

Atmospheric O_2 carries a ^{17}O oxygen isotope anomaly that is isotopically homogenous up to ~80 km[10]. The oxygen isotope anomaly observed in atmospheric O_2 is a function of atmospheric CO_2 levels or the global primary production (GPP)[13–15]. The ^{17}O depletion of air O_2 counterbalances the ^{17}O enrichment of stratospheric O_3 and CO_2. The larger the stratospheric CO_2 reservoir, the larger the negative anomaly of O_2. Anomalous O_2 is diluted by isotopically normal O_2 from photosynthesis, i.e., the anomaly of O_2 becomes smaller with increasing GPP. The triple oxygen isotope composition of air O_2 hence is a proxy for the size of the atmospheric CO_2 reservoir (i.e., CO_2 mixing ratio) or GPP.

[1]Geoscience Center, University of Göttingen, Göttingen, Germany. [2]Institute of Geosciences, Ruhr-University Bochum, Bochum, Germany. [3]School of Physical Sciences, The Open University, Milton Keynes, UK. [4]Dipartimento di Scienze della Terra, Università di Pisa, Pisa, Italy. [5]Leibniz University Hannover, Institute of Earth System Sciences (Mineralogy section), Hannover, Germany. ✉e-mail: fabian.zahnow@uni-goettingen.de

Variations in the oxygen and iron isotope ratios are expressed with the δ notation with Vienna Standard Mean Ocean Water (VSMOW) as reference scale for oxygen and IRMM-14 for iron isotopes[16] (Eq. 1). Equation 1 can equally be written for $\delta^{17}O$ as well as for $\delta^{56}Fe$ and $\delta^{57}Fe$ with ^{54}Fe in the denominator of the isotope ratio expressions.

$$\delta^{18}O^{\text{sample}}_{\text{reference}}(‰) = 10^3 \times \left(\frac{\left(\frac{^{18}O}{^{16}O}\right)_{\text{sample}}}{\left(\frac{^{18}O}{^{16}O}\right)_{\text{reference}}} - 1 \right) \quad (1)$$

Deviations in $\delta^{17}O$ from a reference line are expressed in the $\Delta'^{17}O$ notation (Eq. 2). For $\Delta'^{17}O$, we use a reference line (RL) with a slope of $\lambda_{RL} = 0.528$ and zero intercept[17–19]. Similarly, Eq. 2 can be used to express deviations from the correlated relation of $\delta^{56}Fe$ and $\delta^{57}Fe$ ($\Delta'^{56}Fe$ notation). We use the high-temperature approximation for triple iron isotope equilibrium fraction as a reference line with $\lambda_{RL} = 0.678$ for $\Delta'^{56}Fe$[20].

$$\Delta'^{17}O^{\text{sample}}_{RL} = 10^3 \times \ln\left(\frac{\delta^{17}O^{\text{sample}}_{\text{VSMOW}}}{10^3} + 1\right) - \lambda_{RL} \times 10^3 \times \ln\left(\frac{\delta^{18}O^{\text{sample}}_{\text{VSMOW}}}{10^3} + 1\right) \quad (2)$$

Modern I-type cosmic spherules have $\delta^{18}O$ values up to 57‰ and $\delta^{56}Fe$ up to 45‰[10–12]. Reported $\Delta'^{17}O$ and $\Delta'^{56}Fe$ of modern spherules vary between −0.5‰ and −0.8‰ and −0.05‰ and −0.18‰, respectively[10,11]. No such combined triple oxygen and iron isotope data have been published on fossil I-type cosmic spherules yet. This is due, on the one hand, to a lack of analytical precision in $\Delta'^{17}O$ analysis of established techniques for samples as small as fossil I-type cosmic spherules with diameters predominantly <200 µm. On the other hand, it is not known whether widely abundant chemical and mineralogical diagenetic alteration of fossil I-type cosmic spherules[4,5] also affects their oxygen and iron isotope composition.

Here, we report triple oxygen and iron isotope data of fossil I-type cosmic spherules that were collected from sedimentary rocks of Silurian to Miocene age (~411–7 Ma). We present a technique for the combined analysis of oxygen and iron isotopes of small samples. We also provide details of a non-destructive technique on the identification of diagenetic alteration in a large set of cosmic spherules. We evaluate the isotopic results for their potential to reconstruct past atmospheric $\Delta'^{17}O$, CO_2 levels, or GPP, and compare their precision and significance to established CO_2 proxies.

Results and discussion

Spherule characteristics and isotopic compositions

In total 92 micrometeorites were extracted from six sediments from different localities spanning the Carboniferous to Cretaceous periods. In addition, eight micrometeorites from existing collections[4,5,21] were included in the study, extending the investigated time span from Silurian to Quaternary periods (Supplementary Table S1). All micrometeorites are I-type cosmic spherules. The spherules have diameters between 18 and 429 µm (Supplementary Table S2). The estimated masses of individual spherules, based on their diameters and assumed bulk density of 5 g cm^{-3} [22], range from 0.02 to 103 µg with a median mass of 0.2 µg.

The I-type cosmic spherule exteriors show characteristic dendritic textures and no signs of terrestrial alteration in the secondary electron images (Fig. 1). The samples´ surface mineralogy, determined with the Energy Dispersive X-ray detector (EDX), is composed of Fe oxides. Nickel is present in two Miocene spherules with 1.80 wt% (MDC-D4) and 4.28 wt% (MDC-A5) and Cretaceous spherule SUT11-3 with 0.52 wt% (Supplementary Table S3). Cobalt is abundant in one Carboniferous spherule with 0.50 wt%. Chromium is present in two Permian spherules and three Cretaceous spherules with concentrations between 0.08 wt% and 0.78 wt%. Manganese is detectable from the surface EDX analyses in ~50% of the analyzed I-type cosmic spherules with abundances between 0.21 wt.% and 1.85 wt.%.

The triple oxygen isotope composition was determined for one modern (MA-9) and 20 fossil I-type cosmic spherules large enough for individual analysis (>1 µg[23]). The results are listed in Table 1. Modern sample MA-9 was split into several aliquots to match the small mass of the individual fossil spherules. The investigated I-type cosmic spherules show two distinct patterns of triple oxygen isotope variations (Fig. 2). Most samples cluster between 2.8‰ and 10.0‰ in $\delta^{18}O$, with a $\Delta'^{17}O$ of −0.48‰ to -0.08‰ referred hereafter as the low $\delta^{18}O$ population. A second group comprising of five I-type cosmic spherules scatter in a wider range with elevated $\delta^{18}O$ between 21.9‰ and 54.0‰ and $\Delta'^{17}O$ values between −1.54‰ and −0.03‰. Four of the high- $\delta^{18}O$ specimens, including one modern, one Miocene and two Cretaceous spherules, fall on an extrapolated linear triple oxygen isotope trend described by modern Antarctic I-type cosmic spherules. Miocene sample MDC-D4 and Cretaceous sample SUT11-3 have triple oxygen isotope compositions in the range of unaltered modern specimens ($\delta^{18}O$ = 39–48‰, $\Delta'^{17}O$ = −0.5 to −0.8‰, Fig. 2). Cretaceous sample SUT16-1 is on an extended range of the trend described by modern I-type cosmic spherules with a $\delta^{18}O$ of 21.9 and a $\Delta'^{17}O$ of −0.03‰. The Miocene sample MDC-A5 has a distinctively low $\Delta'^{17}O$ of −1.54‰, deviating from the trend of modern Antarctic I-type cosmic spherules with an offset of −0.83‰.

The triple iron isotope composition was determined for one modern (MA-9) and 12 fossil I-type cosmic spherules that were large enough for individual analysis (Table 1). A majority of the I-type cosmic spherules cluster around 0‰ in $\delta^{56}Fe$, $\delta^{57}Fe$ and $\Delta'^{56}Fe$ (Fig. 3). Four I-type cosmic spherules, including one modern, two Miocene and one Cretaceous specimen, show enriched $\delta^{56}Fe$ and $\delta^{57}Fe$ of 12.1‰ to 34.6‰ and 18.0‰ to 51.7‰, respectively. The four heavily fractionated I-type cosmic spherules follow a linear trend described by modern Antarctic I-type cosmic spherules[11] in the $\Delta'^{56}Fe$ versus $\delta^{57}Fe$ space with $\Delta'^{56}Fe$ values down to −0.26‰ (Fig. 3). The $\Delta'^{56}Fe$ of the isotopically heavy fossil I-type cosmic spherules is compatible with Rayleigh-type evaporation of Fe and FeO and Graham's law kinetic fractionation[24] with no back-reaction between the spherule and the evaporated gas[11] and thus indicative of a preserved primary atmospheric signal.

The diagenetic alteration of cosmic spherules

The presence of Mn in I-type cosmic spherules is diagnostic of diagenetic terrestrial alteration[4]. Manganese should be absent in the Fe-oxides as extraterrestrial metal does not contain any lithophile Mn[25]. Leaching of Ni, Cr and Co, otherwise occurring in detectable amounts in pristine I-type cosmic spherules, is accompanied by implantation of lithophile cations such as Mn, but also Na, Mg, Al and Si[4]. We demonstrated that the Mn to Fe ratio can be readily determined with non-destructive micro X-ray fluorescence (Supplementary Fig. S1). Micro X-ray fluorescence can be utilized to investigate a large number of spherules for terrestrial alteration (i.e., Mn/Fe > 5×10^{-2}) in a time- and resource-efficient manner. The investigated samples in this study show that terrestrial Mn is common in fossil I-type cosmic spherules, independent of host rock lithology and residence time (Supplementary Table S3). The enrichment of Mn is thus likely driven by the abundance of Mn in diagenetic pore fluid.

Fossil I-type cosmic spherules fall into two groups. A small group preserved atmospheric high $\delta^{18}O$ and $\delta^{56}Fe$, with elevated Ni and no detectable Mn. A large group shows low $\delta^{18}O$ and $\delta^{56}Fe$ and elevated Mn (Supplementary Fig. S2). The iron isotope composition of Mn-bearing I-type cosmic spherules investigated here indicates complete mobilization and replacement of extraterrestrial Fe with terrestrial from diagenetic fluids, accompanied with terrestrial values around 0‰ in $\delta^{56}Fe$, $\delta^{57}Fe$[26,27] and $\Delta'^{56}Fe$ (Fig. 3). Thus, the strong enrichment in heavy iron isotopes ^{56}Fe and ^{57}Fe seen in pristine I-type cosmic spherules (occurring during evaporation in the atmosphere) is not preserved in diagenetically altered specimens.

The $\delta^{18}O$ and $\Delta'^{17}O$ variations in the low- $\delta^{18}O$ population can be explained by mixing of inherited primary atmospheric O_2 with oxygen obtained from equilibration with terrestrial fluids (Fig. 2). The degree of oxygen exchange between unaltered and altered endmembers was estimated

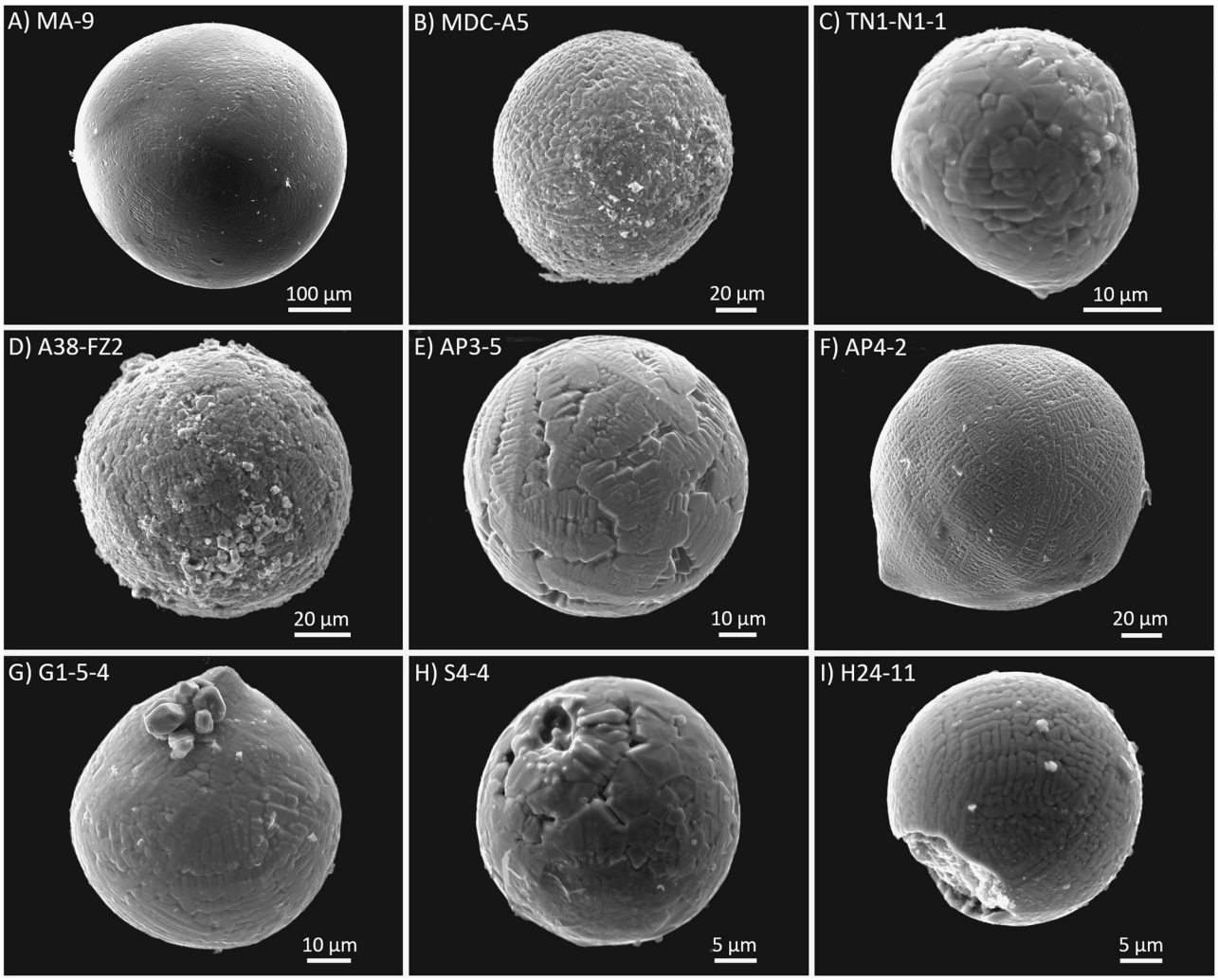

Fig. 1 | Scanning electron microscope secondary electron images of I-type cosmic spherules. Displayed are nine of the investigated spherules, exhibiting different types of larger and smaller external dendritic textures. The figure shows samples from the modern Antarctic sedimentary trap (**A**), Miocene marl (**B**), Cretaceous lime marl (**C**), Triassic paleosoil (**D**), Triassic arkosic sandstone (**E**, **F**), Permian Halite (**G**, **H**), and Carboniferous Limestone (**I**). The images were taken prior to the cleaning procedure for oxygen isotope analysis. Some samples show fragments of the host sedimentary rocks sticking at the surface (**B**, **C**, **D**, **I**).

with a reconstruction of the mixing curve[28] between hydrosphere-equilibrated Fe-oxides and original, evaporated atmospheric Fe-oxides. Under equilibrium low-T conditions there is little oxygen isotope fractionation between magnetite and water[29,30]. Among the diagenetically altered fossil I-types the degree of exchange of oxygen by oxygen from meteoric water ranges from 65% to 90%. The observation of oxygen exchange with pore fluid is consistent with recrystallization of magnetite from primary wüstite in a terrestrial diagenetic setting[4].

We conclude that triple oxygen and iron isotopes can be utilized to assess the proportions of atmospheric signals that are still preserved in the low $\delta^{18}O$ population despite chemical alteration (traced by Mn enrichment).

Reconstructing ancient atmospheric oxygen isotope compositions and paleo-CO_2 levels

We identified four fossil I-type cosmic spherules that entirely preserved their original (from atmospheric interaction) oxygen and iron composition (no Mn enrichment and high $\delta^{18}O$ and $\delta^{56}Fe$). These unaltered fossil I-type cosmic spherules are the Late Miocene samples MDC-A5 and MDC-D4 (~8.5–6.9 Ma) and late Cretaceous samples SUT11-3 and SUT16-1 (~87 Ma). The samples fall on the $\delta^{18}O$ versus $\delta^{56}Fe$ trend described by modern, unaltered I-type cosmic spherules (Fig. 4A). The relation of $\Delta'^{17}O$ and $\delta^{56}Fe$ of the high- $\delta^{18}O$ specimens agrees closely with the kinetic fractionation trend described by modern I-type cosmic spherules (Fig. 4B). Sample SUT16-1 has a lower $\delta^{18}O$, $\Delta'^{17}O$ and $\delta^{56}Fe$ than the other three samples, suggesting low grades of evaporation at atmospheric entry. The good agreement with modern, unaltered spherule entry dynamics indicate that the oxygen in the spherules sources from the Miocene (MDC-A5 and MDC-D4) and Cretaceous (SUT11-3 and SUT16-1) Earth atmosphere. However, Miocene sample MDC-A5 falls off the trend and shows a very low $\Delta'^{17}O$ (−1.54‰), which we relate to the analytical uncertainty of that sample with ~65% blank contribution (average blank = 44%). We therefore exclude this sample from further discussion on the atmospheric composition, although it otherwise appears structurally, chemically and isotopically (except $\Delta'^{17}O$) pristine. The $\delta^{18}O$ (45.4‰) and $\delta^{56}Fe$ (25.5‰) of MDC-A5 match well within the distribution of other unaltered I-type cosmic spherules (Fig. 4A).

Unaltered fossil I-type cosmic spherules can be used to derive the $\Delta'^{17}O$ of ancient atmospheric O_2 and, consequently, to constrain past pCO_2 or GPP at these time intervals. Modern pristine I-type cosmic spherules fall on a linear trend in the triple oxygen isotope space ($\Delta'^{17}O$ versus $\delta^{18}O$, Fig. 2) with a slope of $\lambda = 0.4995 \pm 0.0003$ (1SD) and an intercept of 0.57 ± 0.13‰ (1SD)[11]. The slope is defined by the atmospheric entry processing (kinetic evaporation and oxygen exchange) of the cosmic spherules, which we assume to be similar for modern and fossil specimens. The intercept of the regression function is expected to shift with shifting $\Delta'^{17}O$ of atmospheric O_2 (modern $\Delta'^{17}O = -0.432$‰[18]). With this approach, it is possible to

Table 1 | Triple oxygen and triple iron isotope composition of investigated I-type cosmic spherules

Sample ID	Geologic period	$\delta^{17}O$ (‰)	$\delta^{18}O$(‰)	$\Delta'^{17}O$ (‰)	$\delta^{56}Fe$ (‰)	$\delta^{57}Fe$ (‰)	$\Delta'^{56}Fe$ (‰)
MA-9	Quaternary	27.1	54.0	−1.03	33.9	50.7	−0.19
MDC-A5	Miocene	22.1	45.4	−1.54	25.5	38.3	−0.26
MDC-D4	Miocene	24.8	49.2	−0.81	34.6	51.7	−0.18
SUT11-3	Cretaceous	21.1	41.2	−0.46	12.1	18.0	−0.04
SUT16-1	Cretaceous	11.5	21.9	−0.03	0.0	0.1	−0.02
SUT-C1	Cretaceous	–	–	–	0.8	1.2	−0.03
A38-FZ2	Triassic	3.0	6.5	−0.43	−0.2	−0.2	−0.06
AP1-1	Triassic	4.0	7.7	−0.08	–	–	–
AP1-2	Triassic	2.0	6.1	fil.	–	–	–
AP2-1	Triassic	3.7	7.3	−0.18	–	–	–
AP2-2	Triassic	3.3	8.0	fil.	0.1	0.1	0.06
AP2-3	Triassic	–	–	–	−0.5	−0.7	−0.05
AP2-4	Triassic	–	–	–	−0.3	−0.4	−0.06
AP3-2	Triassic	2.3	4.7	−0.22	–	–	–
AP3-4	Triassic	4.9	10.0	−0.33	–	–	–
AP3-5	Triassic	4.3	7.4	fil.	–	–	–
AP3-6	Triassic	2.1	5.2	fil.	–	–	–
AP4-1	Triassic	3.4	6.8	−0.21	–	–	–
AP4-2	Triassic	3.8	7.7	−0.31	−0.1	−0.1	−0.02
AP4-3	Triassic	4.2	8.7	−0.41	–	–	–
AP4-4	Triassic	2.5	5.1	−0.14	–	–	–
AP5-2	Triassic	2.0	2.8	fil.	–	–	–
AP8-2	Triassic	4.0	8.6	−0.48	–	–	–
G1-5-4	Permian	–	–	–	0.1	0.4	−0.11
SUT22-1	Silurian	3.7	7.3	−0.20	0.3	0.5	−0.02

The symbol "–" denotes not analyzed values and "fil." denotes $\Delta'^{17}O$ filtered for an O_2 amount <10 nmol. $\delta^{17}O$ and $\delta^{18}O$ reported against VSMOW, $\Delta'^{17}O$ relative to a reference line with a slope of 0.528 and zero intercept. $\delta^{56}Fe$ and $\delta^{57}Fe$ reported against IRMM-014, $\Delta'^{56}Fe$ relative to a reference line with a slope of 0.678 and zero intercept. Uncertainties are: $\delta^{17}O$ = 0.3‰ (1SD), $\delta^{18}O$ = 0.6‰ (1SD), $\Delta'^{17}O$ = 0.08‰ (1SD), $\delta^{56}Fe$ = 0.8‰ (2SD), $\delta^{57}Fe$ = 1.3‰ (2SD), $\Delta'^{56}Fe$ = 0.04‰ (2SD).

reconstruct the $\Delta'^{17}O$ of ancient atmospheric O_2 directly, even from the isotope composition of a single fossil I-type cosmic spherule that has preserved its primary atmospheric signal (Eq. 3).

$$\Delta'^{17}O_{0.528}^{\mathrm{atm.O_2}} = \Delta'^{17}O_{0.528}^{\mathrm{spherule}} + 0.0285 \times \delta^{18}O^{\mathrm{spherule}} - 1.005‰ \quad (3)$$

Using Eq. 3, the modern Antarctic I-type cosmic spherule from this study (MA-9) yields a value of -0.49 ± 0.08‰ for $\Delta'^{17}O$ of atmospheric O_2, which is in good agreement with direct measurements of -0.432‰[18]. The reconstructed paleo-atmospheric $\Delta'^{17}O$ values for the investigated unaltered fossil spherules are −0.29 ± 0.08‰ for Cretaceous samples SUT11-3, −0.41 ± 0.08‰ for SUT16-1 and −0.42 ± 0.08‰ for Miocene MDC-D4.

The $\Delta'^{17}O$ of paleo-atmospheric O_2 provides information about pCO_2 and/or GPP (Eq. 4)[11,13]. For the paleo-pCO_2, we first adopt published GPP estimates[31]. The pCO_2 is further depending on the atmospheric pO_2 to pCO_2 ratio[13]. A 50% decrease in pO2 from the modern value of 21% is reflected in a decrease of the atmospheric O_2 $\Delta'^{17}O$ by -0.13‰[13]. A −0.13‰ lower $\Delta'^{17}O$ of atmospheric O_2 would result in a ~300 ppmv higher pCO_2 at a constant GPP (Eq. 4). In this study we apply the paleo-pCO_2 reconstruction on Quaternary to Cretaceous spherules, periods with relatively stable pO_2 compared to the modern value[32]. Possible fluctuations of the pO_2 in the range of ±5% do not affect the pCO_2 reconstruction above the analytical precision (±180–370 ppmv [1SD]). We thus apply Eq. 4 to the atmospheric O_2 $\Delta'^{17}O$ with using the models modern day pO_2 estimate[13]. The paleo-pCO_2 reconstruction based on the $\Delta'^{17}O$ of spherules older than the Jurassic would need an adaption of the model Eq. 4 is based on[13] to account for higher or lower paleo-pO_2.

$$\begin{aligned} pCO_2(\mathrm{ppmv}) = &-7.768 \times \mathrm{GPP} + 0.005 \times \mathrm{GPP}^2 - 300.810 \\ &\times \Delta'^{17}O^{\mathrm{atm.O_2}} - 288.273 \times \left(\Delta'^{17}O^{\mathrm{atm.O_2}}\right)^2 - 22.219 \\ &\times \mathrm{GPP} \times \Delta'^{17}O^{\mathrm{atm.O_2}} - 28.668 \end{aligned} \quad (4)$$

Using Eq. 4, the modern Antarctic I-type cosmic spherule MA-9 suggests a pCO_2 of 417 ± 180 ppmv (1SD), consistent with pre-industrial CO_2 levels of 280 ppmv. The millennium-long residence time of atmospheric O_2 prevents the anthropogenic rise in pCO_2 from immediately impacting modern atmosphere's $\Delta'^{17}O$[13]. The pCO_2 reconstruction of MA-9, supported by published data on Antarctic I-type cosmic spherules[10,11], validates the overall approach. However, the interpretation of the reconstructed pCO_2 data is challenged by the relatively large uncertainty resulting from analyzing such small samples in the lowest microgram range for their $\Delta'^{17}O$ (±0.08‰ [1SD], resulting in pCO_2 ± 180–370 ppmv).

Miocene spherule MDC-D4 with an age of ~8.5 Ma[4] yields a pCO_2 of 294 ± 220 ppmv. Cretaceous specimens SUT13-11 and SUT16-1 with terrestrial residence ages of ~87 Ma[5] suggest pCO_2 levels of $-40\ ^{+360}_{-0}$ ppmv and 500 ± 370 ppmv. The average pCO_2 from the two 87 Ma Cretaceous spherules is $230\ ^{+250}_{-230}$ ppmv.

Significance of the reconstructed CO_2 levels

All reconstructed paleo-atmospheric CO_2 levels, based on the $\Delta'^{17}O$ of I-type cosmic spherules, agree within uncertainty with existing proxy data (LOESS fit)[33] and CO_2 level models (GEOCARBSULF)[34,35] at the respective time intervals (Fig. 5). The spherule, proxy and model data indicate moderate CO_2 levels in modern times (<2 Ma) as well as 10 and 90 million years ago.

The analytical precision of this dataset is ±0.08‰ for the $\Delta'^{17}O$ of iron oxides as small as 1 µg (10 nmol O_2), resulting in pCO_2 reconstructions with an uncertainty between ±180 and ±370 ppmv. The precision of the $\Delta'^{17}O$ analysis dominates the reconstruction precision because it is directly translated into the precision of the reconstructed $\Delta'^{17}O$ of atmospheric O_2 (Eq. 3), which in turn provides information on the atmospheric CO_2 reservoir (pCO_2) and bio productivity (GPP).

Existing proxy collections include $\delta^{13}C$ in liverworts, alkenones (phytoplankton) or paleosols, leaf stomata density and index of land plants and boron isotopes in foraminifers[33,36,37]. The pCO_2 uncertainty in this study (±180–370 ppmv) is of the same magnitude of the average uncertainty of existing proxies for the Miocene and Cretaceous, which range from $^{+120}_{-70}$ ppmv in the Miocene to $^{+380}_{-150}$ ppmv for the Upper Cretaceous[33,36,37]. The weakness of most existent proxies is that they become less available and increasingly imprecise (several thousand ppmv) with geological age and increasing pCO_2 (Fig. 5). The biological and geochemical pCO_2 proxy uncertainties result, next to diagenetic loss of bio-geochemical tracers, from model dependent error estimates that are strongly influenced by calibration of fossil measurements to modern counterparts and imprecise input parameters of transfer functions[33,38]. Corresponding fits (LOESS) based on these proxies, therefore, become increasingly imprecise and are not used for time intervals older than 420 million years (i.e., Devonian).

Our study shows the feasible reconstruction of pCO_2 from the $\Delta'^{17}O$ of a single, intact I-type cosmic spherule across various time intervals (Miocene

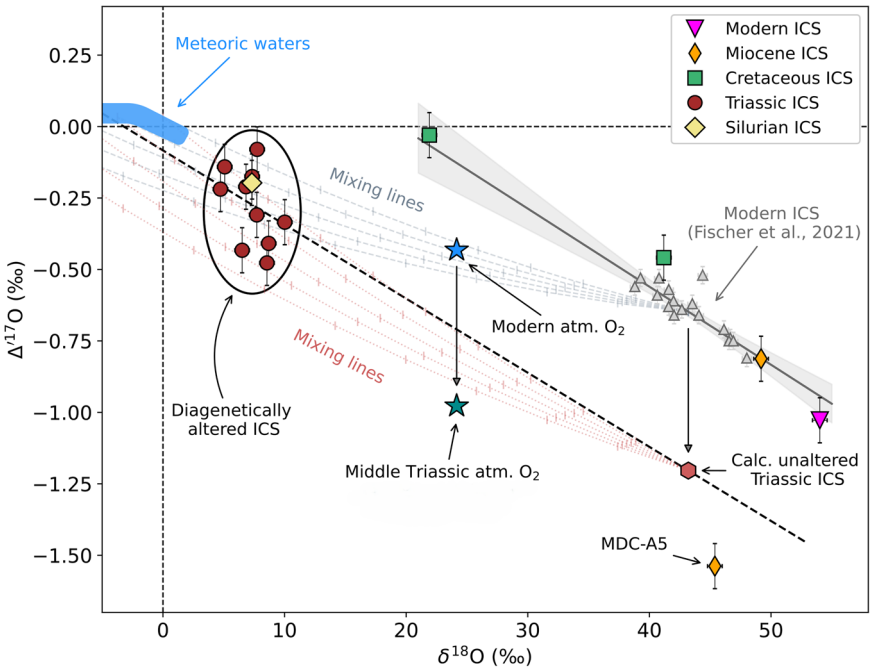

Fig. 2 | Plot of the $\Delta'^{17}O$ versus $\delta^{18}O$ of the I-type cosmic spherules (ICS). The linear regression (gray solid line) is defined by modern I-type cosmic spherules[11]. The majority of fossil spherules are diagenetically altered (black ellipse). The gray-blue dashed curves represent equilibration of oxygen from specimens with modern oxygen isotope composition and oxygen from different meteoric waters[54]. The brown-red dotted curves represent equilibration of oxygen from spherules with a presumed unaltered oxygen isotope composition (brown-red hexagon) with oxygen from meteoric waters[54], indicating a lower $\Delta'^{17}O$ of the Middle Triassic atmosphere (cyan star). The vertical lines of both equilibration line types indicate 10% intervals. Error bars and envelopes are 1SD.

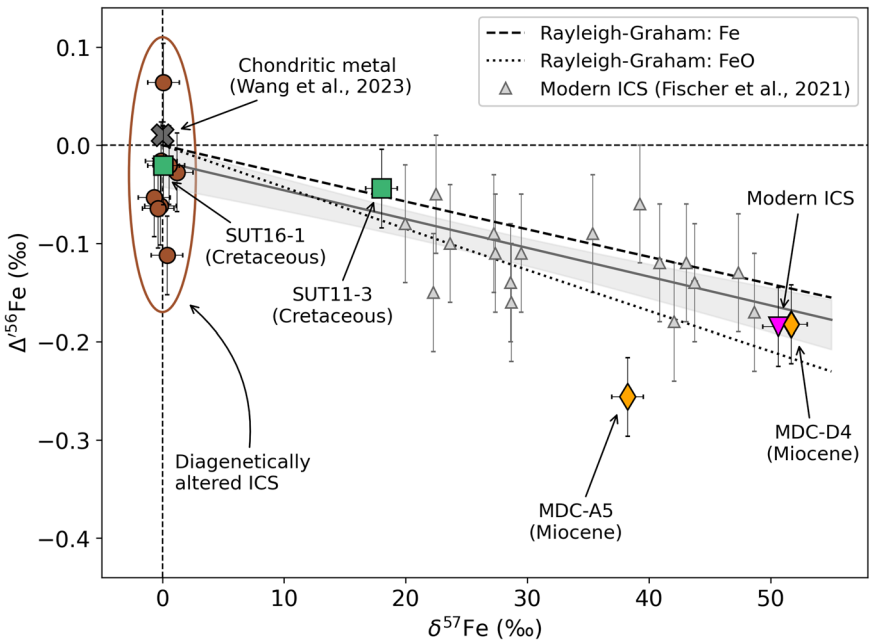

Fig. 3 | Plot of the $\Delta^{56}Fe$ versus $\delta^{57}Fe$ of investigated I-type cosmic spherules (ICS). Modern Antarctic I-type cosmic spherules from the literature[11] are presented as reference (gray triangles). The composition of chondritic metal[26] is depicted as the presumed precursor of I-type cosmic spherules. The slope of the regression line described by modern specimens (gray solid line) can be explained by Graham's law fractionation for Rayleigh-type evaporation of Fe (dashed line) and FeO (dotted line) as described in detail by Fischer et al.[11]. Error bars are 2SD.

and Cretaceous) with a consistent precision of < ± 400 ppmv. This degree of precision should extend throughout the entire Phanerozoic and even throughout the Precambrian, given the enduring geological preservation of I-type cosmic spherules, with the oldest record of unaltered I-type cosmic spherules dating back to 2.7 Ga[3].

Potential and limitations of the atmospheric proxy

The oxygen isotope analytical method used in this study suits samples as small as 1 µg or 10 nmol of O_2, challenging the analytical limits of the laser fluorination technique for micrometer-sized cosmic spherules[23]. The ~1 µg samples allow for an external reproducibility of ±0.04‰ for $\Delta'^{17}O$[23], close to the 0.03‰ internal precision of a gas-source isotope ratio mass spectrometer (Supplementary Fig. S3), potentially reducing the pCO_2 reconstruction uncertainty to ±90–185 ppmv compared to ±180–370 ppmv reported in this study.

Carbonate rocks are currently the sole source of I-type cosmic spherules unaffected by terrestrial weathering[3–5], a conclusions supported our findings. Targeting carbonate host rocks can yield larger populations of pristine spherules, notably reducing uncertainty in pCO_2 reconstructions, as larger sample quantities allow for considerably improved precision. For instance, sampling 10 pristine spherules could achieve an average $\Delta'^{17}O$ uncertainty better than 0.025‰, leading to pCO_2 reconstructions of ~50 ppmv, irrespective of the examined time interval.

We demonstrated that even diagenetically altered fossil I-type cosmic spherules (low $\delta^{18}O$-population) remain useful for paleo-atmosphere reconstruction, because they still contain some oxygen (10 – 35%) of

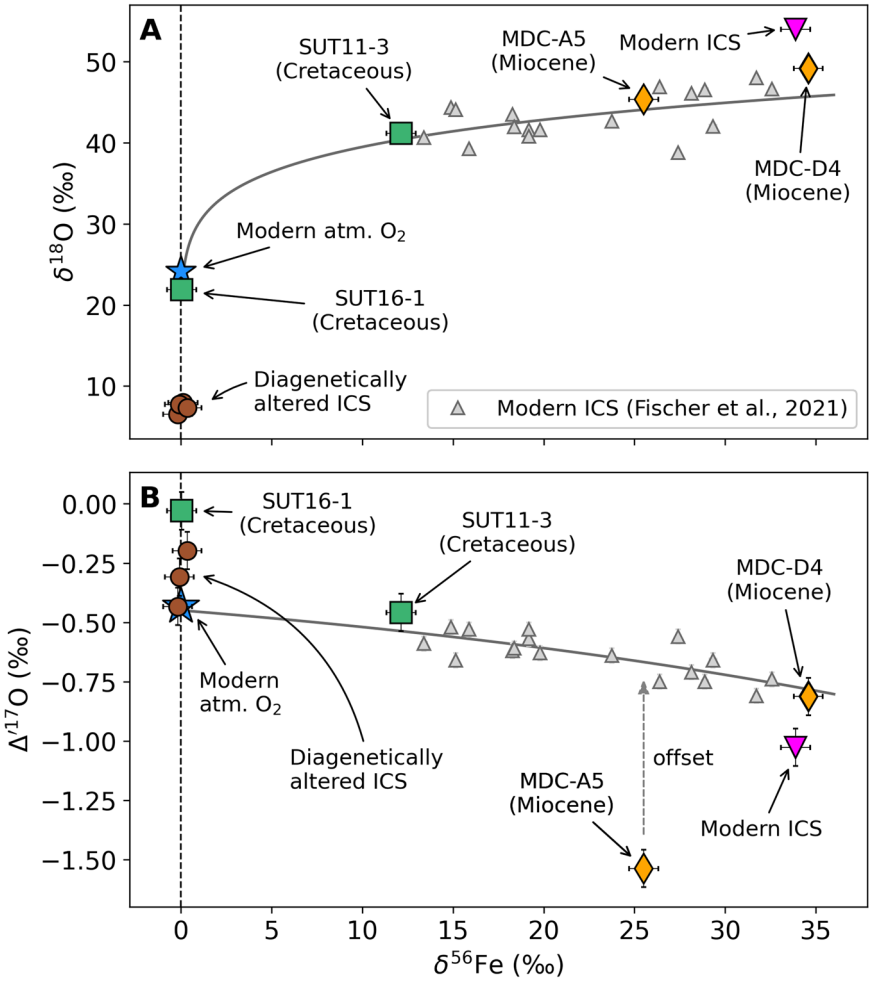

Fig. 4 | Plots of the oxygen isotope composition versus the δ^{56}Fe of I-type cosmic spherules. Displayed are the $\delta^{18}O$ (**A**) and $\Delta'^{17}O$ (**B**) versus δ^{56}Fe of the spherules investigated in this study, together with modern I-type cosmic spherules that are displayed as ref. 11 (gray triangles). The relation between oxygen and iron isotopes of modern I-type cosmic spherules from Fischer et al.[11] is represented as gray solid curves. The oxygen isotope composition of modern atmospheric O_2 is shown for comparison at a pre-evaporative δ^{56}Fe of 0‰. The vertical offset of sample MDC-A5 in $\Delta'^{17}O$ (**B**) is depicted with a grey dashed arrow. Error bars for oxygen isotopes are 1SD and for δ^{56}Fe they are 2SD.

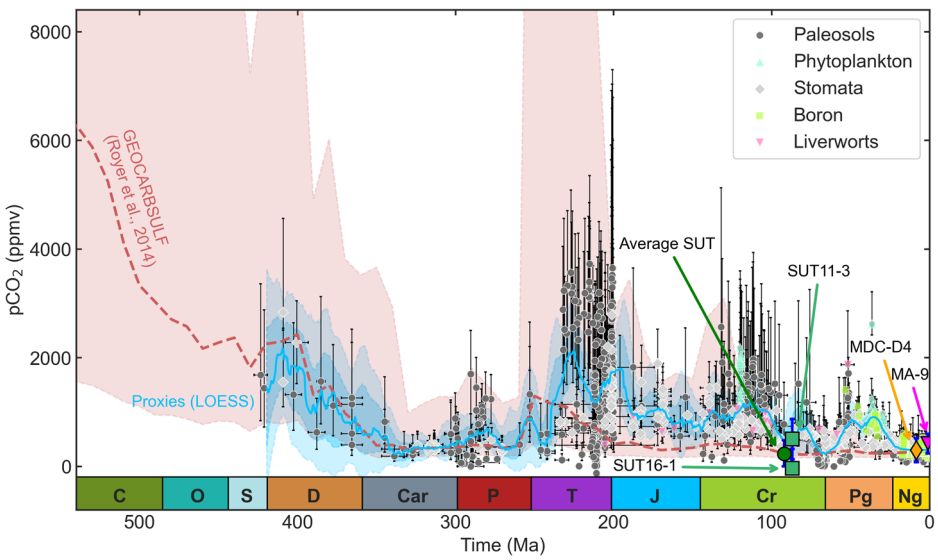

Fig. 5 | Reconstruction of paleo-atmospheric CO_2 concentrations. Displayed are pCO_2 reconstructions determined in this study based on fossil I-type cosmic spherules (labeled) in comparison to published data throughout the Phanerozoic, reconstructed with proxies[33,36,37] and a mass balance model (GEOCARBSULF)[34,35]. Proxies include $\delta^{13}C$ in liverworts, alkenones (phytoplankton) or paleosols, leaf stomata density and index of land plants and boron isotopes in foraminifers. The light blue trend indicates a 0.5 Myr spaced LOESS fit through the proxy data[33]. The light brown trend shows the GEOCARBSULF mass balance model[34] with an associated uncertainty interval[35]. The 1SD uncertainties of individual proxies are displayed as black error bars. For the I-type cosmic spherules 1SD error bars are displayed in blue. The average SUT data point is marginally shifted along the time axis to avoid overlapping the two source data points (SUT11-3 and SUT16-1).

atmospheric origin. Low $\Delta'^{17}O$ values of altered fossil specimens indicate a lower $\Delta'^{17}O$ of the atmospheric O_2 component. For example, altered Middle Triassic spherules show $\Delta'^{17}O$ values as low as -0.48 ± 0.08‰ (Fig. 2). Accounting for diagenetic influences (i.e., substitution of atmospheric oxygen with oxygen from meteoric water), the unaltered endmember $\Delta'^{17}O$ might be as low as approximately -1.20 ± 0.08‰ (Fig. 2). The investigated Silurian spherule with a $\Delta'^{17}O$ of -0.20‰ is indicative of a higher $\Delta'^{17}O$ of atmospheric O_2 with respect to the Triassic specimens. However, more unaltered spherules should be isolated in order to confirm the conclusion of modern-like $\Delta'^{17}O$ of the Silurian atmosphere.

Pristine fossil I-type cosmic spherules that preserved the entire atmospheric O_2 signal are, however, the primary target for paleo-atmospheric reconstruction. The current analytical capabilities provide pCO_2 estimates from one individual unaltered spherule that are comparable or exceeding other existing CO_2 proxy and model uncertainties especially with increasing geologic age[33–35]. The extraction of unaltered I-type cosmic spherules from 2.7 Ga old carbonates[3] is promising in this context. The oxygen isotope composition of unaltered I-type cosmic spherules has the potential to trace paleo-atmospheric processes further back in time than any other existing proxy.

Methods

Samples

We included I-type cosmic spherules from ten localities in this study (Supplementary Table S1). The sedimentary host rocks include marl, limestone, dolocrete, arkosic sandstone and rock salt (halite). A modern Antarctic I-type cosmic spherule from the TAM collection (sediment trap #65) was included as a reference sample[21]. The I-type cosmic spherules in this study span Silurian to Quaternary ages (Supplementary Table S1), covering a wide range of discrete points within the Phanerozoic Eon[4,5,21,39–44]. Varying amounts of rock between 6 kg and 49 kg were collected from each locality (Supplementary Table S2), depending on the expected number of I-type cosmic spherules in the respective rock type. I-type cosmic spherules from existing collections were also examined in this study[4,5].

Micrometeorite extraction

The I-type cosmic spherules were extracted with methods adjusted to the respective host rocks. We focused on collecting the magnetic fraction of each rock for the subsequent search for I-type cosmic spherules with an optical microscope. The magnetic fraction in all the selected lithologies makes up a small proportion of the total rock mass. Possible I-type cosmic spherules can be concentrated efficiently in small magnetic fraction quantities from a large sample quantity (Supplementary Table S2).

The I-type cosmic spherule candidates were identified microscopically (round shape and dendritic texture) and first mounted on double sided tape. That setup was used for micro X-ray fluorescence (μXRF) investigation of the I-type cosmic spherule candidates. The candidates were subsequently mounted and carbon coated on pin stubs for imaging and chemical analysis of the micrometeorite surfaces under the scanning electron microscope (SEM).

Micro X-ray fluorescence

Geochemical investigations were conducted at the University of Göttingen, Germany. The I-type cosmic spherules were scanned for their Mn to Fe ratio and possible Ni content with a Bruker M4 TORNADO μXRF. The μXRF was equipped with an X-ray tube with a rhodium target. We used the μXRF under low-vacuum conditions of 20 mbar, an acceleration voltage of 50 kV and 200 μA beam current. A minimum spot size of 20 μm and acquisition times of 120 s were selected for analysis. We used precidur® 11SMn30Pb30 steel as reference with a Mn concentration of 1.03 ± 0.02 wt%. We also analyzed nine modern Antarctic I-type cosmic spherules with low Mn concentrations of 0.02 ± 0.02 wt% and Ni concentrations of 2.4 ± 1.4 wt% multiple times within each measurement sequence. The weight percentages were calculated semi-quantitatively using a recent oxide calibration.

Scanning electron microscopy

The SEM analyses were carried out using a JEOL JSM-IT500 InTouchScope™ equipped with a Tungsten source and an Ultim Max EDX detector from Oxford Instruments allowing for semi-quantitative EDX analyses. Analyses were performed under high-vacuum at a working distance of 11 mm. The acceleration voltage was set to 15 kV with a beam current of 20 nA and a focused beam. The SEM was used for the acquisition of secondary electron images of the I-type cosmic spherule candidates as well as EDX spot analysis on their surfaces to investigate the size, texture, mineralogy and chemical composition. The SEM data was used to verify the extraterrestrial origin of the I-type cosmic spherules as well as to identify weathering and diagenetic alteration signatures. The detection limits as well as elemental uncertainties varied between 0.04 and 0.21 wt% for μXRF and SEM measurements. The efficiency of both μXRF and SEM in tracing Mn in I-type cosmic spherules is illustrated in Supplementary Fig. S1.

Oxygen isotope analysis

The samples were removed from the pin holder and stored in individual glass vials in preparation for triple oxygen isotope analysis of the identified I-type cosmic spherules. In order to remove residual glue and sediment sticking at the samples, the spherules were gradually cleaned with acetone, ethanol and pure grade H_2O. The samples were stored overnight in a drying cabinet at 50 °C to remove residual moisture.

We used laser fluorination oxygen extraction and purification in combination with gas chromatography and continuous flow isotope ratio monitoring gas spectrometry (IRMS) for triple oxygen isotope analyses at the University of Göttingen, Germany. For continuous flow IRMS analyses a customized Thermo Scientific™ GasBench II coupled with a Thermo Scientific™ MAT 253 gas source IRMS was used. The oxygen isotope analyses followed the procedure described by Zahnow et al.[23] with adjustments made to improve precision with regard to samples in the lowest microgram mass range (Supplementary Fig. S4).

Data was reduced and corrected according to the procedure for continuous flow IRMS analysis[23]. Aliquots as well as bulk I-type cosmic spherule samples, investigated for their triple oxygen isotope composition, had masses ≥1 μg and calculated oxygen amounts ≥8 nmol. The lower limit of the applied continuous flow IRMS oxygen isotope analysis method is ~10 nmol of O_2[23]. Samples with O_2 amounts <10 nmol experience a non-linear drift in $\Delta'^{17}O$, due to the low signal intensity at the IRMS. We filtered the $\Delta'^{17}O$ for O_2 amounts > 10 nmol in order to acquire a robust data set. We used UWG-2 garnet as our primary standard with $\delta^{18}O_{VSMOW} = 5.75‰$ and $\Delta'^{17}O_{0.528} = -0.059‰$[45,46]. As the matrix matched secondary standard, we used magnetite 070113 with $\delta^{18}O_{VSMOW} = 9.9‰$ and $\Delta'^{17}O_{0.528} = -0.09‰$[11,23,47]. The external reproducibility is reported as 1SD of a single analysis and was adopted for all samples based on 27 UWG-2 garnet and 16 magnetite 070113 analyses between 1 and 9 μg or 13 to 119 nmol O_2 (Supplementary Table S4 and Fig. S5). The external reproducibility in $\delta^{18}O$ was 0.6‰ and in $\Delta'^{17}O$ it was 0.08‰.

Iron isotope analysis

We developed a novel approach by employing wet plasma MC-ICP-MS for Fe fluorides, instead of in situ laser ablation on intact I-type cosmic spherules used in earlier studies[11,48]. Utilizing Fe fluorides remaining after oxygen isotope analysis was crucial due to the low masses of individual fossil I-type cosmic spherules, often approaching or falling below the analytical limit of the continuous flow IRMS method (~1 μg or 10 nmol O_2). The goal was to maximize the analysis of individual micrometeorites by initially utilizing the entire sample mass for oxygen isotope analysis.

Iron fluorides that remained in the sample pits after laser fluorination oxygen extraction were collected and stored in Eppendorf vials. The fluorides were dissolved in 0.5 mL of 9 M HCl for extraction of Fe. The digested samples were taken up in 1 ml of 9 M HCl, and pure Fe fractions were obtained by passing the solution through AG MP-1 (100-200 mesh) resin in 2 ml Bio-Rad® columns[49].

Iron isotope measurements were performed at the University of Hannover, Germany using a Thermo-Finnigan Neptune multi-collector inductively coupled plasma mass spectrometer (MC-ICP-MS). For sample introduction, the instrument was equipped with a quartz glass spray chamber (double pass Scott design), a PFA nebulizer (~100 μl min^{-1} uptake rate, Elemental Scientific), a Ni sampler and a Ni X-type skimmer cone. Masses ^{53}Cr, ^{54}Fe, ^{56}Fe, ^{57}Fe, (^{58}Fe) ^{58}Ni and ^{60}Ni were detected simultaneously following the procedure described in Roebbert et al.[49] and Oeser et al.[50], respectively.

The accuracy and precision of the Fe isotope analysis was monitored using an in-house standard (Fe salt from ETH Zurich, Switzerland). Measured at the intensity above 8 V on ^{56}Fe, the average $\delta^{56}Fe$ and $\delta^{57}Fe$ values of our in-house standard relative to IRMM-014 were −0.74 ± 0.03‰

(mean ± 2SD, $n = 22$) and -1.05 ± 0.06‰ (mean ± 2SD, $n = 22$) respectively, in a good agreement with previously published values ($\delta^{56}Fe = -0.72$‰, $\delta^{57}Fe = -1.06$‰[51–53]). Larger uncertainties of $\delta^{56}Fe = -0.79 \pm 0.21$‰ (mean ± 2SD, n = 6) and $\delta^{57}Fe = -0.92 \pm 0.27$‰ (mean ± 2SD, $n = 6$) occurred for the in-house standard measured at ~3 V (~0.3 ppm Fe) on ^{56}Fe. We excluded micrometeorite data analyzed at lower intensities than 3.5 V on ^{56}Fe, to avoid a non-linear drift in $\Delta'^{56}Fe$.

Test measurements were conducted on Fe fluorides using magnetite standard material (magnetite 070113) and a large modern Antarctic I-type cosmic spherule (MA-9). This allowed us to confirm the efficacy of Fe fluorides for iron isotope analysis and to quantify the fractionation introduced by the laser fluorination oxygen extraction procedure (Supplementary Table S5 and Fig. S6). The resulting uncertainty from the Fe fluoride procedure on iron isotope analyses is larger than the internal analytical errors derived from the Fe in-house standard. We adopted the 2SD uncertainty of fluoride measurements of magnetite 070113 standard with $\delta^{56}Fe = 0.9 \pm 0.8$‰ (mean ± 2SD, $n = 6$), $\delta^{57}Fe = 1.4 \pm 1.3$‰ (mean ± 2SD, $n = 6$) and $\Delta'^{56}Fe = -0.02 \pm 0.04$‰ (mean ± 2SD, $n = 6$) for all samples. The uncertainties in $\delta^{56}Fe$ and $\delta^{57}Fe$ are correlated, thus the uncertainty in $\Delta'^{56}Fe$ is smaller. The determined iron isotope values for magnetite 070113 are in good agreement with published values from laser-ablation MC-ICP-MS measurements ($\delta^{56}Fe = 0.86$‰, $\delta^{57}Fe = 1.26$‰, $\Delta'^{56}Fe = 0.00$‰[11]).

Data availability

The chemical and oxygen and iron isotope data that support the findings of this study are available in the Göttingen Research Online data repository with the identifier https://doi.org/10.25625/M0BRRB.

Received: 3 May 2025; Accepted: 2 July 2025;
Published online: 23 July 2025

References

1. Rubin, A. E. & Grossmann, J. N. Meteorite and meteoroid: new comprehensive definitions. *Meteorit. Planet. Sci.* **45**, 114–122 (2010).
2. Love, S. G. & Brownlee, D. E. Heating and thermal transformation of micrometeoroids entering the Earth's atmosphere. *Icarus* **89**, 26–43 (1991).
3. Tomkins, A. G. et al. Ancient micrometeorites suggestive of an oxygen-rich Archaean upper atmosphere. *Nature* **533**, 235–238 (2016).
4. Suttle, M. D. et al. Fossil micrometeorites from Monte dei Corvi: searching for dust from the Veritas asteroid family and the utility of micrometeorites as a palaeoclimate proxy. *Geochim. Cosmochim. Acta* **355**, 75–88 (2023).
5. Suttle, M. D. & Genge, M. J. Diagenetically altered fossil micrometeorites suggest cosmic dust is common in the geological record. *Earth Planet. Sci. Lett.* **476**, 132–142 (2017).
6. Taylor, S. & Brownlee, D. E. Cosmic spherules in the geologic record. *Meteoritics* **26**, 203–211 (1991).
7. Onoue, T., Nakamura, T., Haranosono, T. & Yasuda, C. Composition and accretion rate of fossil micrometeorites recovered in Middle Triassic deep-sea deposits. *Geology* **39**, 567–570 (2011).
8. van Ginneken, M. et al. Micrometeorite collections: a review and their current status. *Philos. Trans. R. Soc. Lond. Ser. A Math. Phys. Eng. Sci.* **382**, 20230195 (2024).
9. Brownlee, D. E. Cosmic dust: Collection and research. *Annu. Rev. Earth Planet. Sci.* **13**, 147–173 (1985).
10. Pack, A. et al. Tracing the oxygen isotope composition of the upper Earth's atmosphere using cosmic spherules. *Nat. Commun.* **8**, 15702 (2017).
11. Fischer, M. B. et al. I-Type cosmic spherules as proxy for the Δ′ 17 O of the atmosphere—a calibration with quaternary air. *Paleoceanogr. Paleoclimatol.* **36**, e2020PA004159 (2021).
12. Engrand, C. et al. Isotopic compositions of oxygen, iron, chromium, and nickel in cosmic spherules: Toward a better comprehension of atmospheric entry heating effects. *Geochim. Cosmochim. Acta* **69**, 5365–5385 (2005).
13. Young, E. D., Yeung, L. Y. & Kohl, I. E. On the Δ17 O budget of atmospheric O2. *Geochim. Cosmochim. Acta* **135**, 102–125 (2014).
14. Luz, B., Barkan, E., Bender, M. L., Thiemens, M. H. & Boering, K. A. Triple-isotope composition of atmospheric oxygen as a tracer of biosphere productivity. *Nature* **400**, 547–550 (1999).
15. Bender, M., Sowers, T. & Labeyrie, L. The Dole Effect and its variations during the last 130,000 years as measured in the Vostok Ice Core. *Glob. Biogeochem. Cycles* **8**, 363–376 (1994).
16. McKinney, C. R., McCrea, J. M., Epstein, S., Allen, H. A. & Urey, H. C. Improvements in mass spectrometers for the measurement of small differences in isotope abundance ratios. *Rev. Sci. Instrum.* **21**, 724 (1950).
17. Miller, M. F. & Pack, A. Why Measure 17 O? Historical Perspective, triple-isotope systematics and selected applications. *Rev. Mineral. Geochem.* **86**, 1–34 (2021).
18. Pack, A. Isotopic traces of atmospheric O2 in rocks, minerals, and melts. *Rev. Mineral. Geochem.* **86**, 217–240 (2021).
19. Sharp, Z. D. & Wostbrock, J. A. Standardization for the triple oxygen isotope system: waters, silicates, carbonates, air, and sulfates. *Rev. Mineral. Geochem.* **86**, 179–196 (2021).
20. Young, E. D., Galy, A. & Nagahara, H. Kinetic and equilibrium mass-dependent isotope fractionation laws in nature and their geochemical and cosmochemical significance. *Geochim. Cosmochim. Acta* **66**, 1095–1104 (2002).
21. Suttle, M. D. & Folco, L. The extraterrestrial dust flux: size distribution and mass contribution estimates inferred from the transantarctic mountains (TAM) micrometeorite collection. *J. Geophys. Res. Planets* **125**, e2019JE006241 (2020).
22. Feng, H. et al. Internal structure of type I deep-sea spherules by X-ray computed microtomography. *Meteorit. Planet Sci.* **40**, 195–206 (2005).
23. Zahnow, F., Stracke, T., Di Rocco, T., Hasse, T. & Pack, A. High precision triple oxygen isotope composition of small size urban micrometeorites indicating constant influx composition in the early geologic past. *Meteorit. Planet. Sci.* **58**, 1567–1579 (2023).
24. Graham, T. X. V. I. I. On the molecular mobility of gases. *Philos. Trans. R. Soc.* **153**, 385–405 (1863).
25. Nozaki, W., Nakamura, T., Iida, A., Matsuoka, K. & Takaoka, N. Trace element concentrations in iron type cosmic spherules determined by the SR-XRF method. *Antarct. Meteor. Res.* **12**, 199–212 (1999).
26. Wang, K. et al. Homogeneous distribution of Fe isotopes in the early solar nebula. *Meteorit. Planet. Sci.* **48**, 354–364 (2013).
27. Beard, B. L. & Johnson, C. M. High precision iron isotope measurements of terrestrial and lunar materials. *Geochim. Cosmochim. Acta* **63**, 1653–1660 (1999).
28. Herwartz, D. Triple oxygen isotope variations in Earth's crust. *Rev. Mineral. Geochem.* **86**, 291–322 (2021).
29. Zheng, Y.-F. Calculation of oxygen isotope fractionation in metal oxides. *Geochim. Cosmochim. Acta* **55**, 2299–2307 (1991).
30. Levin, N. E., Raub, T. D., Dauphas, N. & Eiler, J. M. Triple oxygen isotope variations in sedimentary rocks. *Geochim. Cosmochim. Acta* **139**, 173–189 (2014).
31. Beerling, D. Quantitative estimates of changes in marine and terrestrial primary productivity over the past 300 million years. *Proc. R. Soc. Lond. B* **266**, 1821–1827 (1999).
32. Mills, B. J., Krause, A. J., Jarvis, I. & Cramer, B. D. Evolution of atmospheric O2 through the phanerozoic, revisited. *Annu. Rev. Earth Planet. Sci.* **51**, 253–276 (2023).
33. Foster, G. L., Royer, D. L. & Lunt, D. J. Future climate forcing potentially without precedent in the last 420 million years. *Nat. Commun.* **8**, 14845 (2017).
34. Berner, R. A. GEOCARBSULF: A combined model for Phanerozoic atmospheric O2 and CO2. *Geochim. Cosmochim. Acta* **70**, 5653–5664 (2006).
35. Royer, D. L., Donnadieu, Y., Park, J., Kowalczyk, J. & Godderis, Y. Error analysis of CO2 and O2 estimates from the long-term geochemical model GEOCARBSULF. *Am. J. Sci.* **314**, 1259–1283 (2014).

36. Royer, D. L., Berner, R. A. & Beerling, D. J. Phanerozoic atmospheric CO2 change: evaluating geochemical and paleobiological approaches. *Earth Sci. Rev.* **54**, 349–392 (2001).
37. Royer, D. L., Berner, R. A., Montañez, I. P., Tabor, N. J. & Beerling, D. J. CO2 as a primary driver of Phanerozoic climate. *GSA Today* **14**, 4 (2004).
38. Beerling, D. J., Fox, A. & Anderson, C. W. Quantitative uncertainty analyses of ancient atmospheric CO2 estimates from fossil leaves. *Am. J. Sci.* **309**, 775–787 (2009).
39. Niebuhr, B. & Reich, M. Exkursion 7. Das Campan (höhere Ober-Kreide) der Lehrter Westmulde bei Hannover. In *Geobiologie 2. 74. Jahrestagung der Paläontologischen Gesellschaft in Göttingen, 02. bis 08. Oktober 2004, Exkursionen und Workshops* (eds Reitner, J., Reich, M. & Schmidt, G.) 193–210 (Universitätsverlag Göttingen: Göttingen, Germany, 2004).
40. Arp, G., Hoffmann, V.-E., Seppelt, S. & Riegel, W. Exkursion 6: Trias und Jura von Göttingen und Umgebung. In *Geobiologie 2. 74. Jahrestagung der Paläontologischen Gesellschaft in Göttingen, 02. bis 08. Oktober 2004, Exkursionen und Workshops* (eds Reitner, J., Reich, M. & Schmidt, G.) 147–192 (Universitätsverlag Göttingen: Göttingen, Germany, 2004).
41. Salger, M. & Schmidt, H. Die Forschungsbohrung Eschertshofen 1981 (Vorläufige Mitteilung). *Geol. Bavarica* **83**, 145–161 (1982).
42. Zhang, Y., Krause, M. & Mutti, M. The formation and structure evolution of Zechstein (Upper Permian) salt in Northeast German Basin: a review. *OJG* **03**, 411–426 (2013).
43. Gebhart, U. Mikrofazies und Paläontologie biogener Karbonate der Unteren Mansfelder Schichten (Oberkarbon, Stefan). *Hallesches Jahrb Geowiss.* **13**, 5–21 (1988).
44. Miller, C. G. Ostracode and conodont distribution across the Ludlow/Pridoli boundary of Wales and the Welsh Borderland. *Palaeontology* **38**, 341 (1995).
45. Miller, M. F., Pack, A., Bindeman, I. N. & Greenwood, R. C. Standardizing the reporting of Δ'17 O data from high precision oxygen triple-isotope ratio measurements of silicate rocks and minerals. *Chem. Geol.* **532**, 119332 (2020).
46. Valley, J. W., Kitchen, N., Kohn, M. J., Niendorf, C. R. & Spicuzza, M. J. UWG-2, a garnet standard for oxygen isotope ratios: Strategies for high precision and accuracy with laser heating. *Geochim. Cosmochim. Acta* **59**, 5223–5231 (1995).
47. Pack, A. & Herwartz, D. The triple oxygen isotope composition of the Earth mantle and understanding $\Delta^{17}O$ variations in terrestrial rocks and minerals. *Earth Planet. Sci. Lett.* **390**, 138–145 (2014).
48. Lampe, S. et al. Decoupling of chemical and isotope fractionation processes during atmospheric heating of micrometeorites. *Geochim. Cosmochim. Acta* **324**, 221–239 (2022).
49. Roebbert, Y. et al. Fractionation of Fe and Cu isotopes in acid mine tailings: modification and application of a sequential extraction method. *Chem. Geol.* **493**, 67–79 (2018).
50. Oeser, M., Weyer, S., Horn, I. & Schuth, S. High-precision Fe and Mg isotope ratios of silicate reference glasses determined in situ by femtosecond LA - MC - ICP - MS and by solution nebulisation MC - ICP - MS. *Geostand. Geoanalytic Res.* **38**, 311–328 (2014).
51. Kiczka, M. et al. Iron speciation and isotope fractionation during silicate weathering and soil formation in an alpine glacier forefield chronosequence. *Geochim. Cosmochim. Acta* **75**, 5559–5573 (2011).
52. Schuth, S., Hurraß, J., Münker, C. & Mansfeldt, T. Redox-dependent fractionation of iron isotopes in suspensions of a groundwater-influenced soil. *Chem. Geol.* **392**, 74–86 (2015).
53. Kusonwiriyawong, C. et al. Isotopic variation of dissolved and colloidal iron and copper in a carbonatic floodplain soil after experimental flooding. *Chem. Geol.* **459**, 13–23 (2017).
54. Surma, J., Assonov, S. & Staubwasser, M. Triple oxygen isotope systematics in the hydrologic cycle. *Rev. Mineral. Geochem.* **86**, 401–428 (2021).

Acknowledgements

This research is funded by the Deutsche Forschungsgemeinschaft (DFG, German Research Foundation)—Project number PA909/25-1. This research is also funded by the European Union. Views and opinions expressed are however those of the authors only and do not necessarily reflect those of the European Union or the European Research Council Executive Agency. Neither the European Union nor the granting authority can be held responsible for them. This work is supported by ERC grant "KinO", Project 101088020. We acknowledge support by the Open Access Publication Funds/transformative agreements of the Göttingen University. The use of equipment in the Göttingen laboratory for correlative Light and Electron Microscopy (GoeLEM) is gratefully acknowledged. D. Kohl is acknowledged for the support with the oxygen isotope analysis. We thank the Bavarian Environmental Agency (Hof, Germany) and Gernot Arp (University of Göttingen, Germany) for providing the Triassic rock core samples. We thank G. Miller (of NHM, London) for the supply of a micropaleontology acid-digestion residue from which the two Silurian fossil micrometeorites were extracted. We thank the Royal Society for fieldwork funding (grant number RGS-R1-221005) which made the collection of Miocene micrometeorites possible. Funding for micrometeorite research at the University of Pisa is facilitated by the Italian Programma Nazionale delle Ricerche in Antartide (PNRA) under grant number PNRA16 00029. Planetary materials study at the University of Pisa is also supported by PRIN2022 Cosmic Dust II, ID# 2022S5A2N7 and ASI-MUR SpaceitUp! ID# 2024-5-E.0 - CUP n. I53D24000060005 projects. Antarctic micrometeorites studied in this work were collected during the 2017 Programma Nazionale delle Ricerche in Antartide (PNRA) expedition. Finally, we thank Alireza Bahadori and Carolina Ortiz Guerrero for editorial handling and the reviewers for their valuable suggestions and comments.

Author contributions

F.Z.: conceptualization, visualization, methodology, investigation, evaluation, writing—original draft, writing—review & editing. M.D.S.: investigation, writing—original draft, writing—review & editing. M.L.: methodology, investigation, writing—original draft, writing—review & editing. S.W.: methodology, writing—review & editing. T.D.R.: methodology, writing—review & editing. L.F.: conceptualization, supervision, writing—review & editing. A.P.: conceptualization, visualization, supervision, writing—review & editing.

Funding

Open Access funding enabled and organized by Projekt DEAL.

Competing interests

The authors declare no competing interests.

Additional information

Supplementary information The online version contains supplementary material available at https://doi.org/10.1038/s43247-025-02541-5.

Correspondence and requests for materials should be addressed to Fabian Zahnow.

Peer review information *Communications Earth & Environment* thanks Guido Jonker and Huiming Bao reviewer(s) for their contribution to the peer review of this work. Primary Handling Editors: Alireza Bahadori and Carolina Ortiz Guerrero. A peer review file is available.